Carbohydrate Research, 244 (1993) 225–236
Elsevier Science Publishers B.V., Amsterdam

A small-angle X-ray scattering study of the absorption of water into the starch granule

Ruth E. Cameron * and Athene M. Donald

Cavendish Laboratory, University of Cambridge, Madingley Road, Cambridge CB3 0HE (United Kingdom)

(Received March 9th, 1992; accepted December 16th, 1992)

ABSTRACT

Analysis of the shape of the small-angle X-ray scattering (SAXS) intensity profiles obtained from suspensions of wheat starch granules in water gives information on the amount of absorption into the different regions of the granule. At room temperature, less water is absorbed into the granules the higher the starch concentration. At 51°C, the beginning of the gelatinisation region, lower amounts of water are absorbed when the concentration of starch is high and there is less loss of crystalline order. In an excess of water, co-operative melting occurs, whereas, with less water, the absorption is insufficient to destabilise the crystalline order. The beam damage at room temperature is reflected in a slight increase in order, possibly due to rearrangement after chain scission.

INTRODUCTION

The presence of a single peak in the small-angle X-ray scattering (SAXS) intensity profile obtained from starch was reported first by Sterling[1]. Until recently, this peak has been interpreted in terms of the Bragg formula for scattering from planes of point scatterers. However, it has been shown[2] that, by utilising the information from the whole intensity profile rather than only the peak position, much information about the structure of starch can be obtained. We now report an extension of this approach in a study of the way water is absorbed into the starch granule and its effects on gelatinsation in limiting and excess water.

Of the amylose [(1 → 4)-linked α-D-glucan] and amylopectin [(1 → 4),(1 → 6)-linked α-D-glucan] components of the starch granule, it is thought that the latter is largely responsible for crystalline order. Amylopectin has regions that contain many branch points alternating with unbranched regions[3]. Only segments of unbranched chains will form double helices which, in turn, will pack together to form crystalline regions that can be characterised with wide-angle X-ray scattering

* Corresponding author.

(WAXS). This phenomenon results in alternating lamellae of crystalline and amorphous material. From the results of enzymatic studies[3,4], it has been calculated that the thicknesses of the crystalline lamellae form a fairly broad distribution centred on a thickness of ~ 60 Å.

However, in some starches, this semi-crystalline structure is not present throughout the starch granule. As a wheat starch granule develops, there are fluctuations in the rate or mode of the deposition of starch, which result in the presence of growth rings that can be viewed by various techniques. When hydrated, these growth rings that can be viewed by various techniques. When hydrated, these growth rings may be visible by optical microscopy[5]. Chemically or enzymatically eroded granules viewed by scanning electron microscopy (SEM) clearly show shells which differ in their resistance to attack[6] and may also be seen by transmission electron microscopy, particularly after treatment with acid[7–9]. The rings arise from concentric layers of alternating high and low refractive index, density, crystalline order, and resistance to chemical attack. The width of a high density layer is estimated[10] to be in the range 1200–4000 Å. The high density layers can be identified with the semi-crystalline lamellar structure described above. Therefore, the lower density material in a growth ring must be due to regions of amorphous material (see Fig. 1). In the wheat starch granule, one growth ring is formed per day, and the different modes of deposition of the starch are due to the daily fluctuations of light and temperature that result in fluctuating amounts of available carbohydrate.

The SAXS profile obtained from wheat starch (Fig. 2) is a consequence of the entire structure, with the alternating lamellae of amorphous and crystalline material (shown in Fig. 1) giving rise to the familiar peak in the X-ray pattern at $q \sim 0.06$ Å^{-1}. The differences in electron density between the different types of material strongly affect the shape of the intensity profile. The changes in the SAXS intensity profile of starch which occur as a result of gelatinisation in excess water can be modelled[2] by considering the changes in the electron densities of the different components within the starch granule. In this way, the water being absorbed into, and polysaccharide being leached from, the granule together with the accompanying losses of crystalline order can be observed.

By modelling the SAXS data from wheat starch slurries of various concentrations, gelatinisation in limiting and excess water has been studied. The degree and mode of the absorption of water and the loss of crystalline order give insight into the gelatinisation process, and the results can be compared with those obtained in the literature by DSC.

THEORY

The model used has been described in more detail[2], is shown in Fig. 1, and is the simplest model attempted which adequately describes the scattering. Lamellae of amorphous and crystalline material alternate and a finite number of these

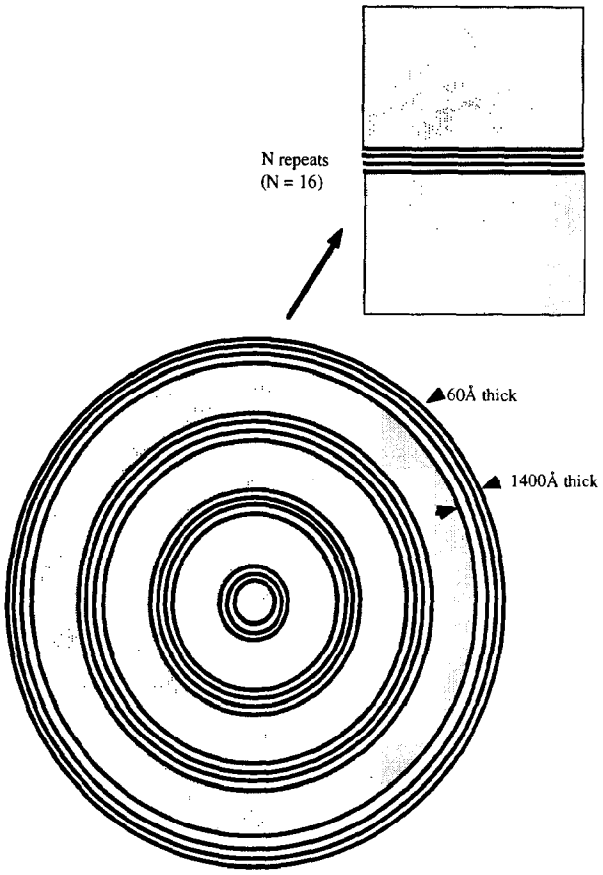

Fig. 1. Schematic representation of the differences in electron density in a starch granule. Regions of alternating lamellae of crystalline and amorphous starch (black and white) are interspersed with amorphous growth rings (dotted). In practice, there would be many more growth rings in a single starch granule. Also shown is the simplified stack used to fit the data, which is infinite in two dimensions, with an infinite background region. A set of randomly oriented stacks is used in the model.

alternating lamellae are taken to represent the high density shell of a growth ring. This finite number of lamellae is then embedded in an infinite medium of a specified electron density (the 'background') which represents the low density shell of a growth ring. Sets of the above structures are then oriented randomly.

This model[2] has six variable parameters. (*1*) The average repeat distance of the amorphous and crystalline material, denoted by d. (*2*) The crystallinity (ϕ), which is the average thickness of the crystalline lamellae divided by d, i.e., the fraction of the alternating lamellae which is crystalline. (*3*) The constant β, related to the widths of the Gaussian distributions of thicknesses of crystalline and amorphous lamellae[11]. (*4*) The number of repeats of alternating crystalline and amorphous lamellae within the high density shell of a growth ring, designated by N. (*5*) The difference in electron density ($\Delta\rho$) between the crystalline and amorphous mate-

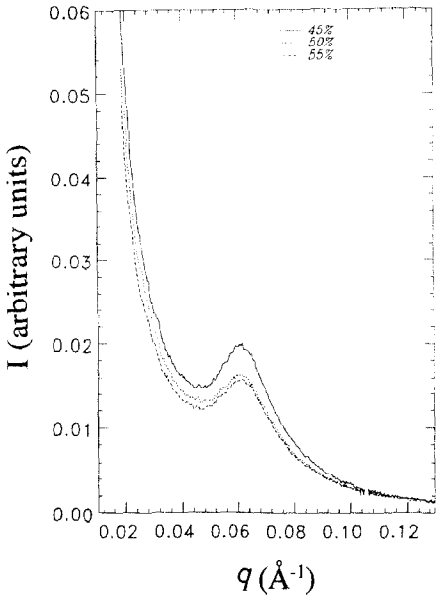

Fig. 2. SAXS intensity profiles of 45, 50, and 55% suspensions of starch in water at room temperature. The exposure time for each curve was 5 min.

rial. (*6*) The difference in election density ($\Delta\rho_u$) between the background and the amorphous material. Thus, if ρ_a, ρ_c, and ρ_u are the electron densities of the amorphous, crystalline, and background material, respectively, then

$$\Delta\rho = \rho_c - \rho_a \text{ and } \Delta\rho_r = \rho_u - \rho_a. \quad (1)$$

Fig. 3 shows the electron density distribution of the model (see ref 2 for the full equation for the scattered intensity).

The changes which take place during gelatinisation can be modelled[2] by varying $\Delta\rho_u$ and $\Delta\rho$ only. Changes in N and d lead to shifts in position of the peak, which is not observed, and changes in ϕ lead only to changes in the high angle region which does not vary much during gelatinisation. Thus, a good approximation involves modelling the changes that are observed in terms of $\Delta\rho_u$ and $\Delta\rho$.

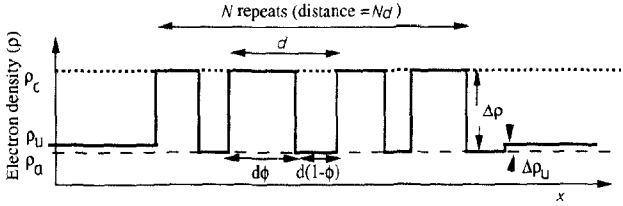

Fig. 3. The electron density distribution profile of the model used. The symbols are defined in the text. The electron density scale is arbitrarily set so that the difference in electron density $\Delta\rho$ is 1 for a 45% slurry of wheat starch in water.

EXPERIMENTAL

Materials.—Slurries (45, 50, and 55% w/w) of wheat starch in water were sealed between two thin mica sheets separated by a brass spacer of width 0.25 mm. The mica was attached to the brass spacer using epoxy resin.

Instrumentation.—Experiments were performed on station 8.2 of the Synchrotron Radiation Source at Daresbury. Data were collected using a quadrant multi-wire detector. The high intensity beam was collimated with slits and focussed onto the detector. The sample-to-detector distance was 3 m and the resulting vertical height of the focussed beam was 0.3 mm. Since the size of the electronic pixels of the detector was 0.4–0.5 mm, no desmearing of the data was necessary. Data were divided by the detector response, normalised with respect to the intensity of the beam exiting the sample, and the background intensity (as recorded from a blanck cell), and a constant liquid scattering term was subtracted for each set. The channel numbers of the detector were mapped onto q values using a wet rat tail collagen calibration. The exposure time for each sample was 5 min.

RESULTS

Variation of the water content a room temperature.—The 45, 50, and 55% slurries of wheat starch in water were exposed at room temperature. Fig. 2 shows the data obtained, which were fitted using the above six parameters. The 45% sample was used as a control in order to determine the value of the y-axis fitting parameter (8.88 for a value of $\Delta\rho$ of 1). The assumption that $\Delta\rho = 1$ arbitrarily fixes the electron density different scale. The value of 8.88 is a conversion factor that is dependent only on the experimental set-up and the value chosen for $\Delta\rho$. Having determined this parameter, however, changes in the value of $\Delta\rho$ can be observed.

The values obtained for the six parameters are shown in Table I. The only parameter which changes to any significant degree with water content is $\Delta\rho$.

The effect of beam damage.—A sample of the 45% slurry was held in the beam at room temperature for 1 h and the data were binned at intervals of 5 min. The results shown in Fig. 4 indicate the effect of beam damage. The data could be

TABLE I

The values obtained from the fits to the SAXS data for starches of different concentrations at room temperature.

Parameter	β	d/Å	ϕ	N	$\Delta\rho_u$	$\Delta\rho$
45% starch [a]	0.34 ± 0.01	89.6 ± 0.8	0.758 ± 0.004	15.9 ± 0.2	0.10 ± 0.06	1.00 ± 0.01
50% starch	0.36	87.2	0.761	16.0	0.08	0.92
55% starch	0.36	88.0	0.748	15.7	0.11	0.90

[a] The results were obtained with four separate samples in order to ascertain the variation.

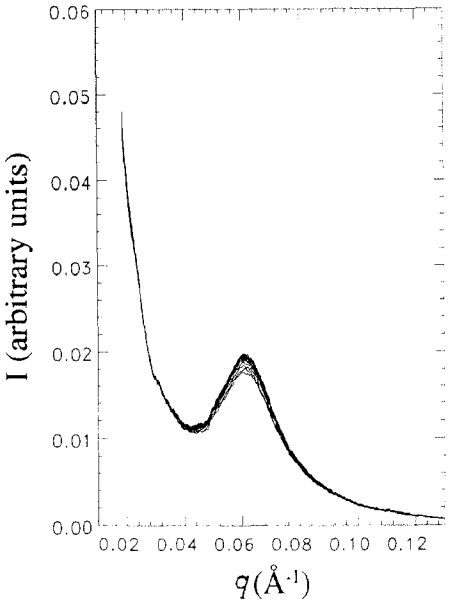

Fig. 4. Changes in the SAXS intensity profile of a 45% slurry of wheat starch in water when it is held at room temperature in the X-ray beam. The counts were binned at intervals of 5 min. The peak sharpens with increasing time.

analysed by varying only $\Delta\rho$ and $\Delta\rho_u$. The other parameters were the same as those found for the 45% slurry held at room temperature for 5 min. The values of $\Delta\rho$ and $\Delta\rho_u$ obtained are plotted in Figs. 5 and 6.

Variation of the water content at 51°C.—Samples of the 45, 50, and 55% slurries were each held in the beam at 51°C for 1 h and the data binned at intervals of 5 min. The data for the 55% slurry are shown in Fig. 7 and were analysed by varying

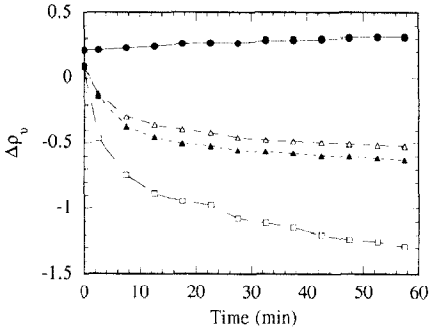

Fig. 5. The calculated values of $\Delta\rho_u$ plotted against time: 45% slurry of starch in water at room temperature (●) and 51°C (□); △, 50% starch at 51°C; ▲, 55% starch at 51°C.

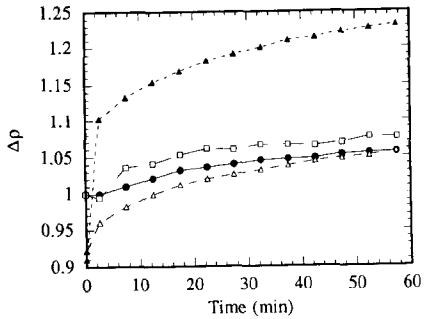

Fig. 6. The calculated values of $\Delta\rho$ plotted against time: 45% slurry of starch in water at room temperature (●) and 51°C (□); △, 50% starch at 51°C; ▲, 55% starch at 51°C.

only $\Delta\rho$ and $\Delta\rho_u$, taking the other parameters to be those obtained at room temperature (Table I). Figs. 5 and 6 show the values of $\Delta\rho$ and $\Delta\rho_u$ obtained.

DISCUSSION

The effect of starch concentration at room temperature.—It is clear from the data in Table I for the 45% slurry of starch in water exposed at room temperature that the greatest uncertainty is in the value of $\Delta\rho_u$ (the difference in electron density between the amorphous and background material). The value of $\Delta\rho$ remains fairly

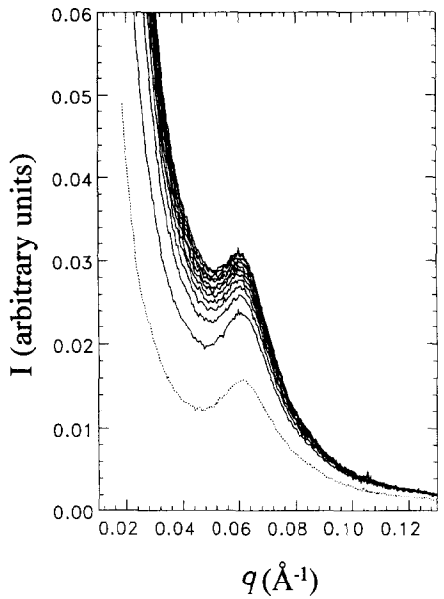

Fig. 7. SAXS intensity profiles of a 55% slurry of starch in water held at 51°C. The counts were binned at intervals of 5 min. Also shown is the profile of the sample at room temperature (dotted line).

constant. There is unlikely to be any difference in the degree of crystalline order between these samples, and hence no change in ρ_c. This situation means that the electron density of the amorphous lamellae ($\rho_a = \rho_c - \Delta\rho$) is unlikely to be changing. Therefore, the changes in $\Delta\rho_u (= \rho_u - \rho_a)$ are likely to be due to changes in the electron density of the background material ρ_u. The most likely reason for this situation is a greater or lesser degree of water absorption into the background material. Thus, it appears that the amount of water absorbed into the background region varies from sample to sample.

The parameters obtained for the 45, 50, and 55% slurries at room temperature are also given in Table I and only the value of $\Delta\rho$ changes significantly. This value [of the difference in electron density between the crystalline and amorphous regions ($\rho_c - \rho_a$)] decreases with decreasing water content. Since there is unlikely to be any difference in the degree of crystalline order between these samples, it seems likely that this effect is due to smaller quantities of water being absorbed into the amorphous layers at lower contents of water. This inference means that the electron density is lowered to a lesser extent and the value of $\Delta\rho$ is correspondingly smaller. Therefore, although all the samples are suspended in water and therefore are hydrated, the more concentrated samples absorb less water. The value of $\Delta\rho_u$ remains roughly the same over the range of concentrations. Since, by the previous argument, the absolute value of ρ_a is probably higher with lower moisture content, the absolute value of ρ_u must be raised similarly, implying that less water is absorbed into the background region as well as into the amorphous lamellae.

Since the absolute value of the electron density of the amorphous lamellae will change from sample to sample as, for example, different amounts of water are absorbed, these experiments give no firm information on the *absolute* values of the electron densities of the different classes of material within the granule. Only the shape of the electron density profile can be determined and position on an absolute scale is not known. However, it is possible to suggest likely positions of these profiles by considering the probable behaviour of the different regions (see below).

The effect of beam damage.—The sample of the 55% slurry held in the beam for 1 h at room temperature gives an idea of the effect of beam damage. It will be seen from Figs. 5 and 6 that the value of $\Delta\rho_u$ increases slightly (from 0.21 to 0.31), as does that of $\Delta\rho$ to a lesser degree (from 1.00 to 1.06). A probable explanation is that beam damage involves limited chain scission, allowing rearrangement of the polysaccharides and subsequent increase in order of both the background and the crystalline material. The background material has more space and potential for ordering and therefore does so to a greater extent than the crystalline layers, which means that $\Delta\rho_u$ increases more than $\Delta\rho$. The amorphous material is still markedly constrained and highly branched, despite some chain scission, and so probably does not increase in order. These effects are illustrated in Fig. 8. Similar effects have been reported for polyethylene, where beam damage from electrons in the

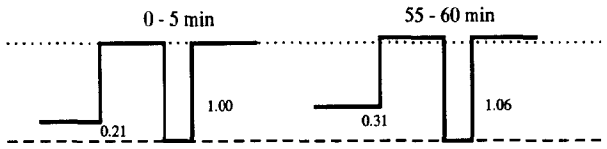

Fig. 8. The effect of beam damage at room temperature on the electron density profiles of a 45% suspension of wheat starch in water. The axes are the the values of ρ_a and ρ_c corresponding to the first 5 min in the beam. Possible positions of these profiles on these axes are shown.

electron microscope induces re-ordering and results in closer packing and an increase in the density of the polymer[12–14].

Starch at 51°C.—It will be seen from Figs. 5 and 6 that, at all concentrations, the trends are the same. The changes are discussed in terms of water ingress, although it is possible that some annealing of the sample may occur. However, the timescale of the experiment (a maximum of 1 h) is appreciably shorter than times over which annealing is usually discussed[15]. The value of $\Delta\rho_u$ becomes increasingly negative with increasing time at 51°C, whereas that of $\Delta\rho$ rises. The rise in $\Delta\rho$ implies that the difference in density between the crystalline and amorphous lamellae ($\rho_c - \rho_a$) increases with time. Since the crystalline regions are unlikely to become more dense during this treatment (apart from small increases due to rearrangement after chain scission caused by beam damage) and may become less dense due to the disruption of order at this elevated temperature, there must be some lowering of electron density (ρ_a) of the amorphous lamellae. This effect is due probably to water being absorbed into the amorphous regions, thereby lowering their electron density. Relative to the lowered value of ρ_a, the value of the background electron density (ρ_u) is reduced still further. This increase in difference in density is probably due to ingress of water into the amorphous growth rings and possibly the leaching of a small amount of amylose from them. Significant leaching of amylose does not occur until ~55°C, according to the literature[16]. The large negative values of $\Delta\rho_u$ indicate that this background region absorbs water and loses amylose to a much greater degree than the amorphous lamellae in the semi-crystalline bulk. This result is because the background material is less constrained and more able to absorb water than the amorphous lamellae. For the same reasons, the chains in this regions are more able to escape from the granule.

The above arguments explain the general changes in shape of the electron density profiles. By considering the behaviour of the suspensions of different concentrations, possible positions of these profiles relative to the values for wheat starch at room temperature can be proposed. The estimated positions[2] of the 45% samples at 51°C can be revised in the light of the new information from different concentrations.

Although the values of $\Delta\rho_u$ and $\Delta\rho$ at the different concentrations change in the same way, there are significant differences in their values. Fig. 9 shows the electron density profiles obtained from the analysis. The value of $\Delta\rho(=\rho_c - \rho_a)$ is

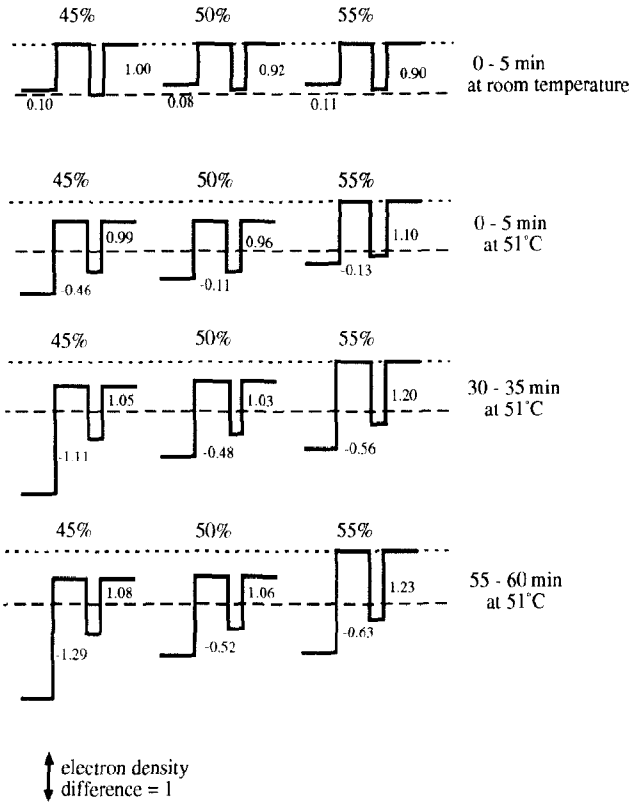

Fig. 9. The changes in the electron density profiles of 45, 50, and 55% suspensions of wheat starch in water at 51°C. The axes are the values of ρ_a and ρ_c for the 45% suspension corresponding to the first 5 min in the beam. Possible positions of these profiles on these axes are shown.

much higher for the 55% sample (1.23) than it is for the 45% sample (1.08). Since the former, which has less water available, is unlikely to have absorbed more water into its amorphous lamellae than the 45% sample, the higher value of $\Delta\rho$ must be due to a lower average degree of disruption of the crystalline lamellae, i.e., not to a lower ρ_a but to a higher ρ_c than the 45% sample. This conclusion suggests that a significant amount of crystalline order has been lost in the 45% sample, which is reflected in its position on the axes in Fig. 9.

The value of $\Delta\rho_u$ is much less negative for the 55% sample (-0.63) than for the 45% sample (-1.29). This difference means that, relative to the lowered values of ρ_a in these samples, the value of ρ_u is lowered further still and to a greater extent in the 45% sample. This finding is to be expected, since there is more water available for absorption in the 45% starch slurry.

Now that the 45 and the 55% samples have been positioned on the axes, the 50% sample can be considered. It seems reasonable to expect the values of ρ_c, ρ_a, and ρ_u to lie at positions between their corresponding values for the 45 and the 55% slurries. This positioning is shown in Fig. 9 which indicates that at 50%, as at

45%, there is considerable loss in crystalline order on raising the temperature to 51°C.

The positions of the electron density distributions at different concentrations follow the same argument at the other times held at 51°C, as shown in Fig. 9. At these shorter times, the values of $\Delta\rho_u$ and $\Delta\rho$ are less extreme than at the final time, but the behaviour is the same.

The trends seen at the different concentrations may be understood in terms of the behaviour reflected by DSC during gelatinisation. At 45%, the starch is in an excess water environment and the DSC gives a single peak (the 'G' peak) at ~ 56°C. At 50 and 55% starch, there are two peaks namely the G peak, which appears at the same temperature, 56°C, and the so-called M1 peak which occurs at higher temperatures. The lower the water content, the higher the temperature at which the M1 peak occurs. At very low contents of water, the G peak is not present.

According to Blanshard's interpretation[17] of the model of Donovan[18,19], the G peak is associated with the absorption of water into the amorphous regions of the starch. When a certain level of absorption is reached, the crystalline regions are destabilised and melt with a co-operative process. In the 45% samples studied here, there is a significant loss of crystalline order at 51°C. This finding may be interpreted as reflecting absorption of water and co-operative melting. According to the model, at lower contents of water, the absorption is not sufficient to destabilise the crystallites to the same degree. Some or all of the crystalline material must be destabilised subsequently via the M1 process. The extent to which loss of order occurs will depend on the water content and the temperature.

It is likely that it is the absorption of water into the amorphous lamellae rather than the background material which is critical in determining the extent of co-operative melting of the crystallites. This material is intimately connected to the crystalline lamellae by the branch points of the amylopectin and thus any disruption of the amorphous lamellae will help to disrupt the crystalline lamellae. By contrast, the background regions are not strongly associated with the crystalline lamellae, and co-operative melting will be less sensitive to the absorption of water.

These considerations can be used to explain the degree of crystalline order lost in the 45, 50, and 55% starch slurries. At 45%, the starch is in excess water and the process of co-operative melting of the crystallites results in a substantial lowering of ρ_c. At 50%, there is still sufficient absorption of water into the amorphous lamellae to lower ρ_c. However at 55%, the crystalline lamellae are much less affected, as the amount of water absorbed into the amorphous lamellae is not sufficient to initiate co-operative melting.

ACKNOWLEDGMENTS

We thank the A.F.R.C. and Dalgety plc for financial support and Professor C.G. Vonk for his advice on the theoretical aspects of the work. The X-ray

experiments were performed with the Synchrotron Radiation Source at the Daresbury Laboratory of the S.E.R.C., with the help and advice of Dr. W. Bras.

REFERENCES

1 C. Sterling, *J. Polym. Sci.*, 56 (1962) S10–S12.
2 R.E. Cameron and A.M. Donald, *Polymer*, 33 (1992) 2628–2635.
3 J.P. Robin, C. Mercier, R. Charbonniere, and A. Guilbot, *Cereal Chem.*, 51 (1974) 389–406.
4 S. Hizukiri, *Carbohydr. Res.*, 147 (1986) 342–347.
5 O.A. Sjostrom, *Ind. Eng. Chem.*, 28 (1936) 63–74.
6 G. Hollinger and R.H. Marchessault, *Biopolymers*, 14 (1975) 265–276.
7 M.S. Buttrose, *J. Cell Biol.*, 14 (1962) 159–167.
8 P. Kassenbeck, *Staerke*, 30 (1978) 40–46.
9 M. Yamaguchi, K. Kainuma, and D. French, *J. Ultrastruct. Res.*, 69 (1979) 249–261.
10 D. French, in R.L. Whistler, J.N. Bemiller, and E.F. Paschell (Eds.), *Starch: Chemistry and Technology*, Academic Press, New York, 1984, pp 183–247.
11 C.G. Vonk, *J. Appl. Crystallogr.*, 11 (1978) 540–546.
12 D.T. Grubb, A. Keller, and G.W. Groves, *J. Mater. Sci.*, 7 (1972) 131–141.
13 D.T. Grubb and A. Keller, *J. Mater. Sci.*, 7 (1972) 822–835.
14 D.T. Grubb, *J. Mater. Sci.*, 9 (1974) 1715–1736.
15 D. Lund, *CRC Crit. Rev. Food Sci. Nutr.*, 20 (1984) 249–273.
16 R.F. Tester and W.R. Morrison, *Cereal Chem.*, 67 (1990) 551–557.
17 J.M.V. Blanshard, in T. Galliard (Ed.), *Starch: Properties and Potential*, Wiley, New York, 1987, pp 16–54.
18 J.W. Donovan, *Biopolymers*, 18 (1979) 263–275.
19 J.W. Donovan and C.J. Mapes, *Staerke*, 32 (1980) 190–193.